



*Supplement of*

## **Modelling seawater $p\text{CO}_2$ and pH in the Canary Islands region based on satellite measurements and machine learning techniques**

Irene Sánchez-Mendoza et al.

*Correspondence to:* Melchor González-Dávila (melchor.gonzalez@ulpgc.es)

The copyright of individual parts of the supplement might differ from the article licence.

## SUPPLEMENTARY MATERIAL

### METHODS

The two VOS have a SBE38 Digital Oceanographic Thermometer (SeaBirdTM), located at the seawater inlet, measuring the sea surface temperature (SST) with high accuracy ( $\pm 0.001^{\circ}\text{C}$ ). The seawater then splits into three lines; the first goes to a set of additional sensors, including an SBE45 Digital Thermosalinograph (accuracy of  $\pm 0.001^{\circ}\text{C}$  and  $\pm 0.0001 \text{ S m}^{-2}$  for temperature and conductivity, respectively) for sea surface salinity (SSS), and an Aanderaa sensor for oxygen. The second seawater line goes to the equilibrator system, located in the wet box of a General OceanicsTM GO8050 automated seawater system and then to the non-dispersive infrared LICOR© analyser for gas detection (models 6262 until 2021 and 7000 later) placed inside the dry box responsible for measuring the molar fraction of CO<sub>2</sub> (xCO<sub>2</sub>, ppm). The analyser is automatically calibrated on departure and arrival at each port and periodically in a loop every three hours using four standard gases (in the order of 0 ppm, 250 ppm, 400 ppm and 550 ppm and with an accuracy of  $\pm 0.02$  ppm). They are provided by the National Ocean and Atmospheric Administration (NOAA) and the ICOS CAL research facilities (after 2022) and traceable to the World Meteorological Organization (WMO). The third seawater line goes out to favor low temperature differences between the intake and the equilibrator. After 2022, the CO<sub>2</sub> equipment on CanOA-VOS-2 was replaced by a membrane CO<sub>2</sub>-PRO FT-ATM (ProOceanusTM), which also uses four calibration gases.

The two moored oceanographic buoys are equipped with several sensors. The sensors integrated in the oceanographic buoys (González et al., 2023) include an SBE 37-SI/SIP MicroCAT thermosalinometer that measures SST and salinity every hour, a Cyclops-7F fluorescence sensor, an Optode 4835 Oximeter and a SAMI-pH pH-meter that measures every three hours. Both buoys contain a ProOceanus pCO<sub>2</sub> PRO-CV monitoring system.

MORGAN-1 also had a Battelle *p*CO<sub>2</sub> monitoring system (years 2020-2021) with a span calibration gas of 534.56 ppm, while ULA-2 includes a SAMI-*p*CO<sub>2</sub> sensor. All *p*CO<sub>2</sub> sensors measure at a frequency of three hours. Measured data is sent to a central data logger, which records all data and sends it to a server via satellite signal.

Figure S1. Longitudinal distribution of the seasonal and annual means of observational SST (top) and satellite-based SST (bottom). Plots on the left correspond to the westernmost part (along the CanOA-VOS-2 track) averaged seasonally and annually at longitudinal intervals of  $0.05^{\circ}$ . Plots on the right are for the easternmost part (along the CanOA-VOS-1 track) averaged at  $0.1^{\circ}$ .

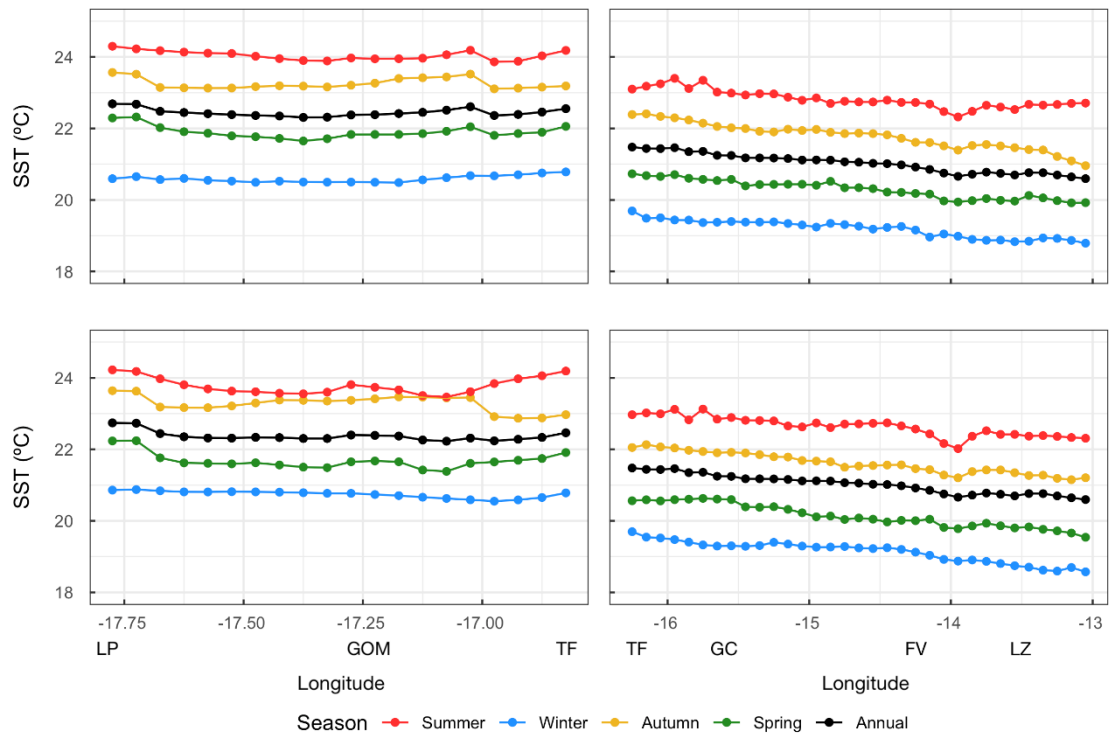


Figure S2. Measured vs. predicted  $p\text{CO}_{2,\text{sw}}$  in the training and validation dataset for the different predictive models containing  $p\text{CO}_{2,\text{atm}} + \text{SST} + \text{Chl } a + \text{MLD}$ .

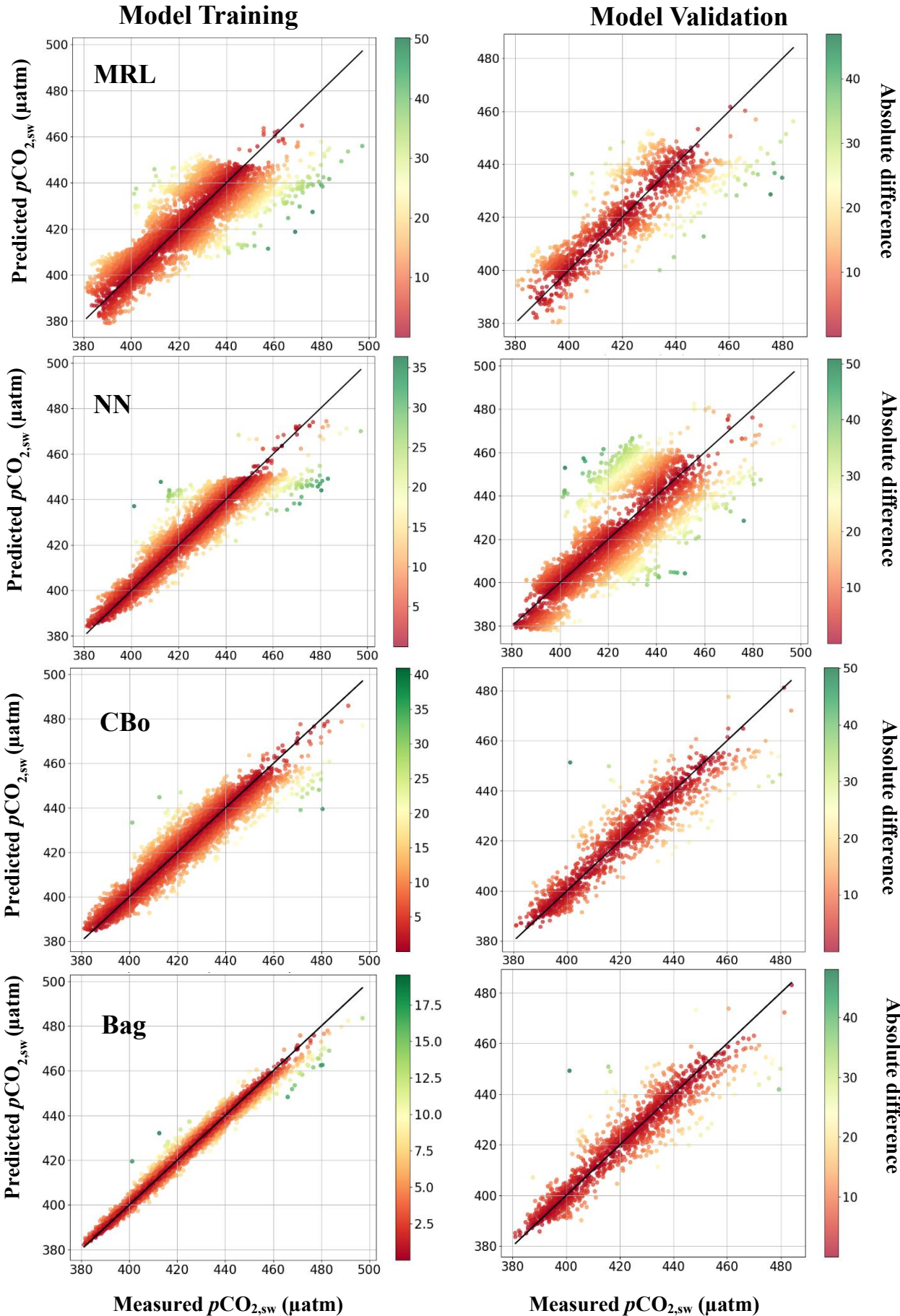


Figure S3. Measured vs. predicted  $\text{pH}_{\text{T,issw}}$  in the training and validation dataset for the different predictive models containing SST + Chl  $\alpha$  + MLD

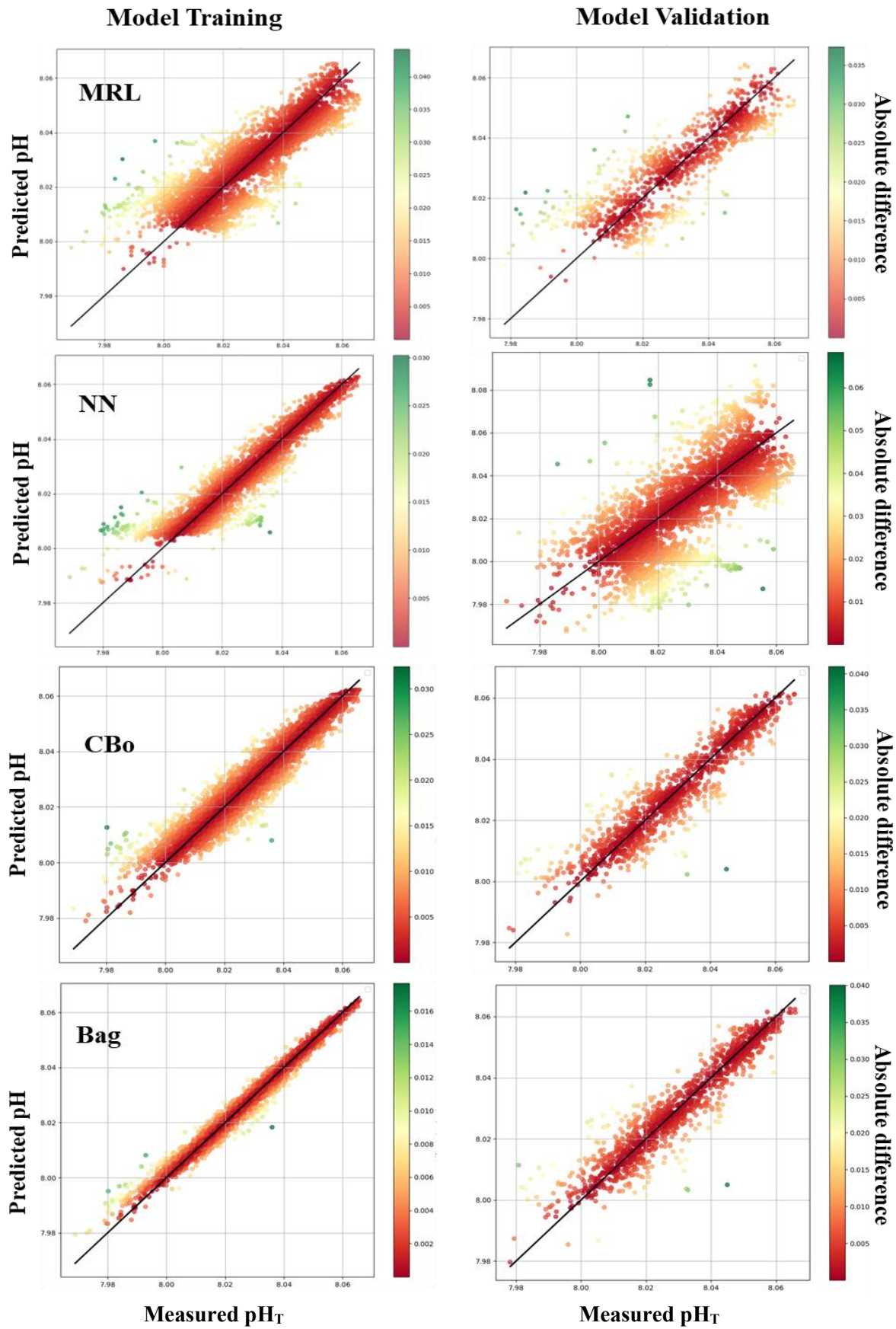


Table S1. Summary of the field data included in the model.

Observing system	Name	Time range	Frequency	Observations
<b>Voluntary Observing Ships vessels (VOS)</b>	Bechinjigua Express	Feb. 2019 – Feb. 2024	Twice a day	208,507
	Jona Sophie (Renate P.)	Feb. 2019 – Feb. 2024	weekly	121,431
<b>Oceanographic buoys</b>	MORGAN-1	Jan. 2020 – Feb. 2024	3-hourly	10,975
	ULA-2	Feb. 2020 – Sep. 2021	3-hourly	1,184

Table S2. Algorithm performance between predicted  $p\text{CO}_{2,\text{sw}}$  ( $\mu\text{atm}$ ) and measured  $p\text{CO}_{2,\text{sw}}$  ( $\mu\text{atm}$ ) for each model using the validation data set.

Algorithm	Variables	R <sup>2</sup>	RMSE ( $\mu\text{atm}$ )	MAE ( $\mu\text{atm day}^{-1}$ )	SSE ( $\mu\text{atm}^2 \text{ day}^{-1}$ )
MLR	SST	0.612	11.2	9.1	22.7
	SST + Chl-a	0.697	10.4	8.2	22.0
	SST + MLD	0.728	10.0	8.1	21.2
	SST + Chl-a + MLD	0.736	10.0	7.9	19.1
	SST + $p\text{CO}_{2,\text{atm}}$	0.759	9.6	7.8	18.7
	<b>SST + Chl-a + MLD + <math>p\text{CO}_{2,\text{atm}}</math></b>	<b>0.802</b>	<b>8.2</b>	<b>7.0</b>	<b>16.7</b>
Neural Network (NN)	SST	0.732	11.8	9.0	27.8
	SST + Chl-a	0.751	11.0	8.8	25.5
	SST + MLD	0.798	10.8	8.1	21.6
	SST + Chl-a + MLD	0.836	8.9	6.1	17.9
	SST + $p\text{CO}_{2,\text{atm}}$	0.836	8.7	6.0	19.1
	<b>SST + Chl-a + MLD + <math>p\text{CO}_{2,\text{atm}}</math></b>	<b>0.862</b>	<b>8.4</b>	<b>5.9</b>	<b>17.9</b>
CatBoost	SST	0.725	10.5	7.6	16.8
	SST + Chl-a	0.819	8.9	6.0	9.6
	SST + MLD	0.836	8.0	5.6	7.7
	SST + Chl-a + MLD	0.914	7.0	4.6	4.9
	SST + $p\text{CO}_{2,\text{atm}}$	0.899	6.2	6.9	5.0
	<b>SST + Chl-a + MLD + <math>p\text{CO}_{2,\text{atm}}</math></b>	<b>0.926</b>	<b>5.9</b>	<b>8.5</b>	<b>4.3</b>
Bagging	SST	0.872	8.9	6.8	5.0
	SST + Chl-a	0.908	8.0	6.0	3.1
	SST + MLD	0.936	5.8	5.4	1.9
	SST + Chl-a + MLD	0.955	5.4	4.0	1.2
	SST + $p\text{CO}_{2,\text{atm}}$	0.937	5.2	4.4	1.7
	<b>SST + Chl-a + MLD + <math>p\text{CO}_{2,\text{atm}}</math></b>	<b>0.955</b>	<b>4.3</b>	<b>3.2</b>	<b>1.1</b>

Table S3. Algorithm performance between predicted and measured  $\text{pH}_{\text{Ti},\text{ssw}}$  for each model using the validation data set.

Algorithm	Variables	R <sup>2</sup>	RMSE	MAE	SSE
MLR	SST	0.678	0.010	0.008	0.067
	SST + Chl-a	0.714	0.009	0.007	0.051
	SST + MLD	0.729	0.009	0.007	0.026
	SST + Chl-a + MLD	<b>0.737</b>	<b>0.008</b>	<b>0.007</b>	<b>0.021</b>
Neural Network (NN)	SST	0.710	0.009	0.008	0.051
	SST + Chl-a	0.725	0.008	0.008	0.028
	SST + MLD	0.739	0.008	0.007	0.022
	SST + Chl-a + MLD	<b>0.818</b>	<b>0.006</b>	<b>0.007</b>	<b>0.013</b>
CatBoost	SST	0.742	0.008	0.006	0.050
	SST + Chl-a	0.821	0.007	0.006	0.007
	SST + MLD	0.853	0.006	0.004	0.010
	SST + Chl-a + MLD	<b>0.893</b>	<b>0.005</b>	<b>0.004</b>	<b>0.003</b>
Bagging	SST	0.879	0.009	0.007	0.017
	SST + Chl-a	0.882	0.007	0.006	0.014
	SST + MLD	0.926	0.005	0.006	0.009
	SST + Chl-a + MLD	<b>0.959</b>	<b>0.003</b>	<b>0.002</b>	<b>0.006</b>

Table S4. AIC computed for the MLR model of  $p\text{CO}_{2,\text{sw}}$ .

Variables	AICc	ΔAICc
SST	127.885	52.654
SST + Chl-a	123.994	48.763
SST + MLD	113.823	38.592
SST + Chl-a + MLD	109.954	34.723
$p\text{CO}_{2,\text{atm}} + \text{SST} + \text{Chl-a} + \text{MLD}$	<b>75.231</b>	<b>0.00</b>

Table S5. AIC computed for the MLR model of  $\text{pH}_{\text{Ti},\text{issw}}$ .

Variables	AICc	$\Delta\text{AICc}$
SST	193.129	0.000
SST + Chl-a	196.109	172.629
SST + MLD	197.860	298.023
SST + Chl-a + MLD	201.856	473.035